Force between charged particles with ion condensation

Peilong Chen[1] and C.-Y. D. Lu[1,2]
[1]*Department of Physics and Center for Complex Systems, National Central University, Chungli 320, Taiwan*
[2]*Department of Chemistry, National Central University, Chungli 320, Taiwan*
(Received 25 June 1999)

We have numerically calculated the interaction forces between two highly charged spherical particles embedded in a cloud of small ions with or without charge redistribution on the particle surfaces. Ion condensation near the charged particles leads to reduced electrostatic interaction between the particles, and we find that the effective two-particle interaction is significantly smaller than the values expected from considering only effective single-particle potentials.

PACS number(s): 52.25.Zb, 61.25.Hq

I. INTRODUCTION

Many interesting physical systems contain large charged particles, sometimes referred to as macroions, that are embedded in a cloud of small ions. The electrostatic forces between the charged particles and the small ions may be dominate in many cases, hence dictate the physical properties of the system. One good example is a system of charged colloidal particles in solutions with or without dissolved salts [1]. Another interesting system is a dusty plasma, in which large charged dust particles interact with the electrons and ions of the background plasma. Dusty plasmas have long been observed in space [2], and more recently in laboratories [3]. Further examples in physical, chemical, and biological systems are numerous [4].

The simplest mean field approach to describe this system is the Poisson-Boltzmann equation (PBE) [5]. A linear approximation of the PBE leads to an electrostatic potential around a macroion of the Debye-Hückel (DH) form, with a characteristic screening length. This effective description has been very successful for weakly coupled particles. For highly charged particles, the current understanding is that some ions will condense near the particle surface, the net particle charge will be reduced, and the remaining ions and electrostatic potential can be treated again within the linear Poisson-Boltzmann equation (LPBE). This is well understood in the case of a line charge, where Manning [6] first systematically demonstrated this condensation by showing that without it, the free energy computed from the partition function will diverge near a highly charged line charge (*Manning condensation*).

In Manning condensation, it is assumed that for a line charge just enough ions will condensate onto it to remove this free energy divergence. On the other hand, one could start from the Poisson-Boltzmann equation and systematically obtain condensation. For a single macroion in one and two dimensions (a charged plane and cylinder, respectively), there exist analytical solutions [7] for the PBE, and indeed condensation is obtained. In three dimension (charged spheres), the PBE can only be solved numerically.

For a mixture of large charged particles and small ions, one of the particularly interesting physical properties is the effective interaction between ''dressed'' particles, under the simplification that small ions are treated adiabatically. Within the assumption of a ''mean spherical'' approximation closure, this interaction has been calculated [8], and shown to be of the Debye-Hückel form with renormalized effective charges. This is consistent with the picture of Manning condensation. Charged colloidal particles in a crystal lattice have also been studied by solving the PBE numerically with the spherical Wigner-Seitz cell approximation [9]. It has been found that the the electrostatic potential is of the DH form near cell boundaries, with effective renormalized charges. An ''*ab initio*'' method that combined equilibrium calculations for the ions with molecular dynamics simulations for macroions was also used to compute macroion properties, with a pseudo-potential technique to avoid the discontinuous behavior of the ionic potential at macroion surfaces [10].

In this paper we present the results of a direct calculation of the interaction between two spherical particles from the Poisson-Boltzmann equation. The results are obtained for both uniform fixed surface charges and moving surface charges yielding a constant electrostatic potential. The PBE is numerically solved and the dependence of the free energy on particle separation is computed. We are particularly interested in studying how ion condensation affects the interaction in the highly charged regime. This problem has been studied before [11], but the charge considered was much lower than that of the present work. They numerically solved the PBE by using a bispherical coordinate system for two spheres. The results thus obtained were then used to benchmark the accuracy of various approximating methods, such as the Deryaguin approximation, the superposition approximation, and the Hogg-Healy-Fuerstenau approximation. However, their results did not clarify the relationship between the two-particle interaction and their charges. More important is the charge renormalization by ion condensation near surface in the limit of high charge, as discussed in the rest of this paper.

At high particle charges, nonlinearity and ion condensation lead to a sharp increase of the electrostatic potentials near the particle surface, thus requiring a very fine grid in the numerical solutions. We thus adopt the usual spherical coordinate system with the origin at the center of one particle, but with nonuniform radial grids. Details of the numerical method are described in Sec. III.

This paper is organized as follows: in Sec. II we briefly review the density functional formulation which we use to

obtain the Poisson-Boltzmann equation and expression of the free energy. Sec. III describes our numerical method. Solutions of the PBE for a single spherical particle are presented in Sec. IV, which will serve as a basis of comparison with two-particle interaction. The results of two-particle interaction are presented in Sec. V.

II. DENSITY FUNCTIONAL FORMULATION

Consider two negatively charged particles embedded in a large system consisting of positive (referred as ions hereafter) and negative (referred as electrons) charges at an average number density n_0 initially. We choose to write the formulation in an open system which is in contact with heat and particle reservoirs of constant temperature and density. The mean field free-energy density functional is thus written as

$$F=T_i\int n_i\ln n_i d\mathbf{r}+T_e\int n_e\ln n_e d\mathbf{r}+\frac{1}{2}\int \phi e n_i d\mathbf{r}-\frac{1}{2}\int \phi e n_e d\mathbf{r}+\frac{1}{2}\int \phi f d\mathbf{r}+\mu_i T_i\int n_i d\mathbf{r}+\mu_e T_e\int n_e d\mathbf{r}.$$

The first two terms are the entropic contributions of ions and electrons. Ions and electrons are assumed carrying charge $\pm e$, and their temperatures are T_i and T_e, respectively. Although, e.g., in colloidal systems where the small ions are moving in a solution T_i is always equal to T_e, in a rf-powered weakly ionized dusty plasma they could be different by a factor of 100 [12]. $n_i(\mathbf{r})$ and $n_e(\mathbf{r})$ are the ion and electron number density, and $f(\mathbf{r})$ represents the charge distribution of the two charged particles. The middle three terms are the total electrostatic energy with $\phi(\mathbf{r})$ the electrostatic potential. μ_i and μ_e are the chemical potentials, and the last two terms are necessary because there are particle exchanges between the system and the reservoirs.

The equilibrium configuration is determined by $\delta F/\delta n_i=\delta F/\delta n_e=0$, with boundary conditions

$$n_i(r\to\infty)=n_e(r\to\infty)\to n_0,\quad \phi(r\to\infty)\to 0.$$

One then recovers the usual Boltzmann distributions,

$$n_i=n_0e^{-e\phi/T_i},\quad n_e=n_0e^{e\phi/T_e},\tag{1}$$

with $\mu_i=\mu_e=-\ln n_0-1$. Inserting these charge distributions into the Poisson equation yields the PBE,

$$\nabla^2\phi=-4\pi(en_i-en_e+f)=-4\pi[en_0(e^{-e\phi/T_i}-e^{e\phi/T_e})+f].\tag{2}$$

We also obtain the free energy as

$$F=\frac{1}{2}\int \phi f d\mathbf{r}-\frac{1}{2}e\int (n_i-n_e)\phi d\mathbf{r}-\int (T_in_i+T_en_e)d\mathbf{r}.$$

Note that in this open system, the last integral will not be a constant. The LPBE follows when ϕ in Eq. (2) is expanded to the lowest order,

$$\nabla^2\phi_l=4\pi e^2n_0\left(\frac{1}{T_e}+\frac{1}{T_i}\right)\phi_l-4\pi f.$$

The corresponding free energy becomes

$$F_L=\tfrac{1}{2}\int \phi_l f d\mathbf{r}-n_0V(T_i+T_e).\tag{3}$$

From the last two equations it is easy to see that, in the linear theory, two charged point particles interact through a screened-Coulomb interaction.

These equations can be written in dimensionless form by defining

$$\frac{1}{T}\equiv\frac{1}{T_e}+\frac{1}{T_i},\quad \eta\equiv\frac{1}{T_e}\Big/\left(\frac{1}{T_e}+\frac{1}{T_i}\right),\quad \lambda^{-2}\equiv\frac{4\pi n_0e^2}{T},$$

and using λ as the length scale, e/T as the electrostatic potential unit, and n_0 as the number density unit. λ is the Debye length which defines the screening length. The total charge of the particle denoted as Q will then be measured in the unit of $en_0\lambda^3$. The particle radius will be denoted by σ in the unit of λ. The resulting PBE and free energy become

$$\nabla^2\phi=e^{\eta\phi}-e^{-(1-\eta)\phi}-f,$$

$$F=\frac{1}{2}\int \phi f d\mathbf{r}-\frac{1}{2}\int (n_i-n_e)\phi d\mathbf{r}-\frac{1}{(1-\eta)}\int n_i d\mathbf{r}-\frac{1}{\eta}\int n_e d\mathbf{r}.$$

For the linear approximation,

$$\nabla^2\phi_l=\phi_l-f,$$

$$F_L=\frac{1}{2}\int \phi_l f d\mathbf{r}-V(T_i+T_e)/\lambda^3T.$$

Here we have used the same symbols for the dimensionless variables, since only the dimensionless equations will be used from now on.

III. NUMERICAL METHODS

We first solve the PBE for a single spherical charged particle. The resulting one-dimensional radial equation is integrated by the standard fourth-order Runge-Kutta method. We choose to integrate starting far away from the origin (the location of the particle) and inward to the particle surface. Integrating from a large distance away (say, 20 Debye lengths) we can safely start from zero potential and match the derivative of potential at the surface to particle charges, which are assumed to uniformly distribute on the surface for a single particle.

In order to solve the PBE, and compute the free energy for a system with two charged spheres, a suitable grid is required. For two identical spheres, symmetry around the axis connecting both centers permits calculations to be done in two dimensions. Symmetry with respect to the bisection plane between the two spheres further reduces the necessary computational domain by half. We thus adopt a spherical

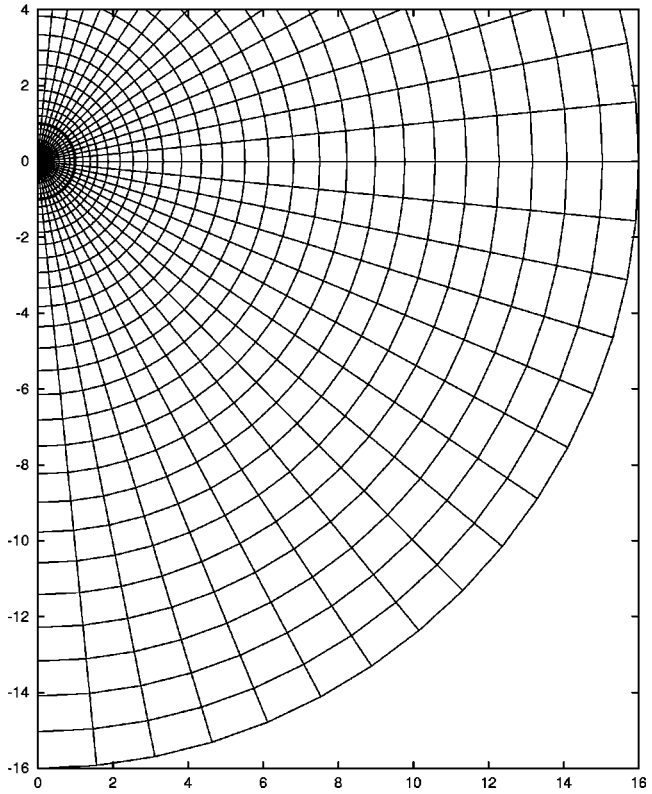

FIG. 1. Grid system used in calculation of two-particle potential. For clarity, grids shown here are fewer than those in the computations.

grid with the origin at the center of one of the spheres, as depicted in Fig. 1 (for the sake of clarity, fewer grid nodes are drawn here than those used in actual computations).

In this paper we consider two types of surface charge behaviors: (1) fixed uniform surface charges such that the potential boundary condition at the surface is implemented as a jump in normal derivative between the two sides of the surface and (2) surface charge redistribution allowed to give a constant surface electrostatic potential. The fixed charge case is, for example, the usual condition for charge colloidal particles where charges mostly come from the ionic molecules embedded on the surface. On the other hand, a constant surface electrostatic potential is more appropriate in dusty plasmas where charges of dusts come mostly from accumulation of free electrons.

Since the coordinate origin is at the center of a particle, the particle boundary (the thick line in Fig. 1) lies at $r=\text{const}$. As illustrated in Fig. 1, grid points in the radial direction are not uniform in order to have a denser grid near the particle surface. In this way, with a manageable number of grid points, we can accurately represent the potential as well as its large derivative near the particle surface, and at the same time cover a large enough computational domain such that the zero potential boundary condition can be used at the domain boundary. Calculations have been made using a range of number of grid points to make sure that the results are independent of the discretizations.

This ability to easily adjust the radial grid is the main motivation to choose the spherical coordinate system with the origin at the particle center. This, however, comes at a price in that a cutting plane, i.e., the midplane between particles, must be drawn at the upper boundary, resulting in an irregular grid points thus complicating the computer coding. At this cutting plane, zero normal derivative boundary condition (with respect to the plane, not to coordinate lines) are implemented to represent the intended situation of two identical particles with a separation twice that of the distance between the origin and this plane. In other words, different interparticle separations are obtained by cutting the plane at different locations.

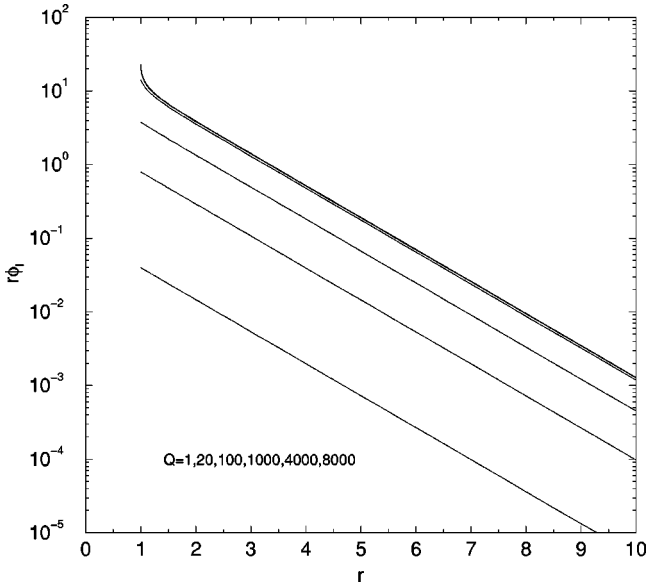

FIG. 2. Single-particle potential from the integration of one-dimensional PBE. From the lowest line up, $Q=1$, 20, 100, 1000, 4000, 8000. Note that the last two lines are almost indistinguishable.

The method of successive-over-relaxation is used to solve the PBE in this grid. In addition, instead of solving the PBE directly, we actually solve the equation for the quantity $\delta\phi \equiv \phi - \phi_l$, with ϕ_l the symmetrical potential for a single particle, which is obtained as mentioned above by integrating the radial PBE. With ϕ_l subtracted out, $\delta\phi$ has much smaller values and derivatives than ϕ, especially at high charges, and hence it is easier to obtain accurate results.

IV. SINGLE-PARTICLE POTENTIAL

In this section we present results for the one-particle potential, ϕ_l, from the integration of the radial PBE to have a systematic account of the potential, and to establish a basis of comparison for our results on two charged particle interactions. Similar results also appeared in [13]. In Fig. 2 the symmetrical potentials outside a charged sphere with unit radius are shown, with values of the particle charge $Q=1$, 20, 100, 1000, 4000, and 8000. The temperature parameter η equals to 0.5, i.e., $T_i = T_e$. Different values of particle radius and η yielded similar results. At $Q=1$ and 20 we see perfect straight lines in the plot of $\log(r\phi_l)$ vs r, i.e., the expected DH potential: $Q\exp(-r)/r$. At $Q=100$, the potential outside the immediate vicinity of particle surface is still of the same form. Near the particle boundary ($r=1$), however, the potential starts to slightly deviate from the DH form. A sharp increase near $r=1$ is apparent for $Q=1000$, and becomes

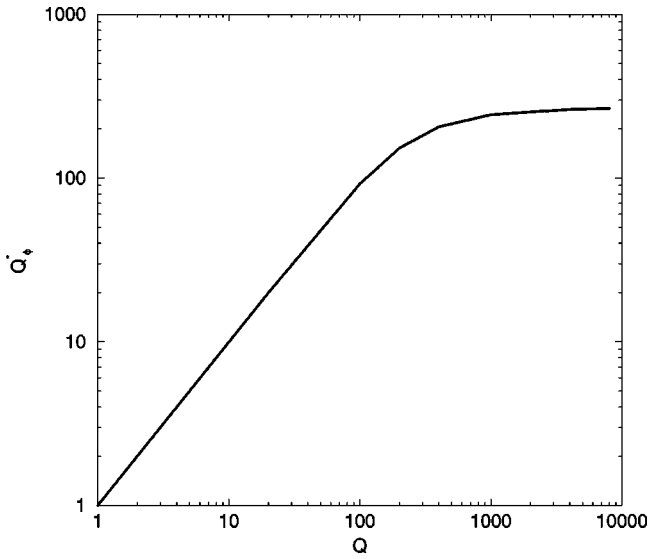

FIG. 3. Effective charge defined from single-particle potential for $\sigma=1$.

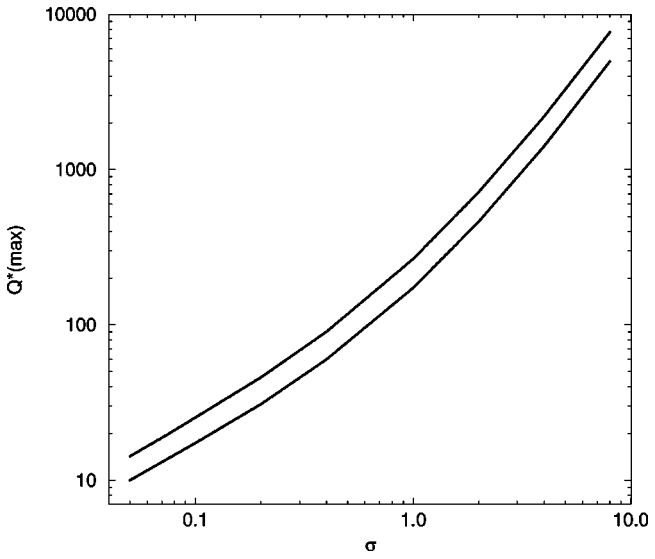

FIG. 4. Maximum effective charges as functions of particle sizes. The upper curve is from the one-particle potential and the lower curve from the two-particle free energy.

more pronounced as Q is further increased.

The sharp increase of potential near the boundary reflects a large concentration of ions, corresponding to condensation. As a consequence of this pileup, there is a reduction and eventual saturation of the far field potential, as clearly demonstrated in the figure. There $\phi_l(Q=4000)$ and $\phi_l(Q=8000)$ are indistinguishable, except very close to the particle surface. Since the potential outside the immediate neighborhood of the particle remains of the screened Coulomb form, we can thus define an effective charge Q_ϕ^* for any value of Q, such that the potential outside is given by $Q_\phi^* \exp(-r)/r$. For $\eta=0.5$ and $\sigma=1$ (the particle radius), the effective charge Q_ϕ^* is plotted in Fig. 3 as a function of the original charge Q. $Q_\phi^*=Q$ for low Q. However, as Q increases over 100, Q_ϕ^* saturates to a upper limit of about 266.

The saturated value, denoted as $Q_\phi^*(\max)$, can only depend on the size of the particle. This dependence is plotted as the upper curve in Fig. 4. From this curve and the size of the particle, we can immediately determine the maximum electrostatic strength from the particle. For example, in the case of a dusty plasma [14], one set of possible parameters is $\lambda \approx 0.1$ mm and the particle size ≈ 5 μm, leading to $\sigma=0.05$. This value of σ gives to a value of $Q_\phi^*(\max)$ of about 14, although estimates of actual total charges on the particle could be much larger [15].

It is reasonable that $Q_\phi^*(\max)$ increases with σ. Scaling as σ^2 at large σ is expected as it should be controlled by the charged particle surface area. This behavior is indeed seen in Fig. 4.

V. TWO-PARTICLE INTERACTION

We next discuss the solutions for two charged particles. Effective charges obtained from the solutions of the radial PBE earlier seem to imply that the interaction will scale as $Q_\phi^{*2} e^{-2d}/2d$, with $2d$ the particle separation. However, we show here that, from two-particle solutions of this finding, Q_ϕ^* overestimates the effective interaction charge by about 40%. The possible implication of this finding for systems of three- and more particle interactions is also discussed.

The idea behind the potential effective charge Q_ϕ^* is that the small condensation region will become inert. However, we find that, based on results here, the condensation region still actively interacts with the other particle. The usefulness of Q_ϕ^* depends on the existence of high charge concentrations in the condensation region. However, these very large charge concentrations and potentials in this region can induce a large effect on the other particle due to the exponential nonlinearity.

The PBE for two spherical particles is solved with the method detailed in Sec. III. The resulting free energy is shown in Fig. 5 with $\eta=0.5$ and $\sigma=0.1$, as a function of interparticle separation for the case of uniform surface charges. At small Q, the linear theory is expected to be cor-

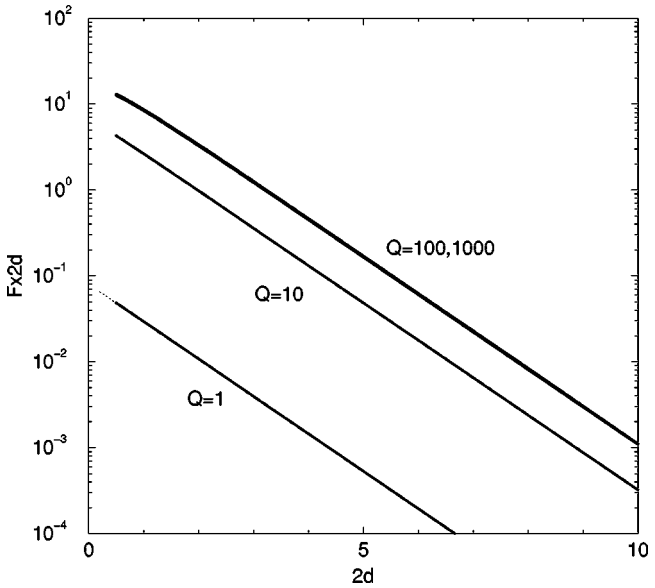

FIG. 5. Two-particle free energy as functions of separation for $\sigma=0.1$ under the uniform surface charge condition. The dash line is the point particle analytical result.

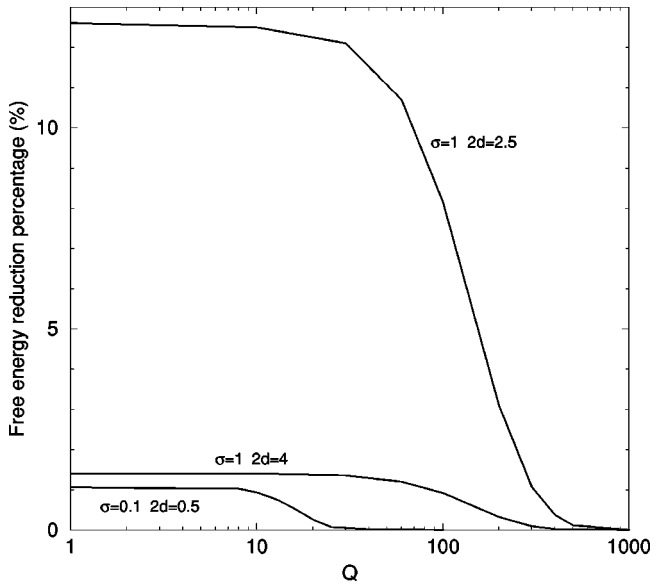

FIG. 6. Reduction percentage of the free energy from the uniform surface charge condition to the constant potential condition.

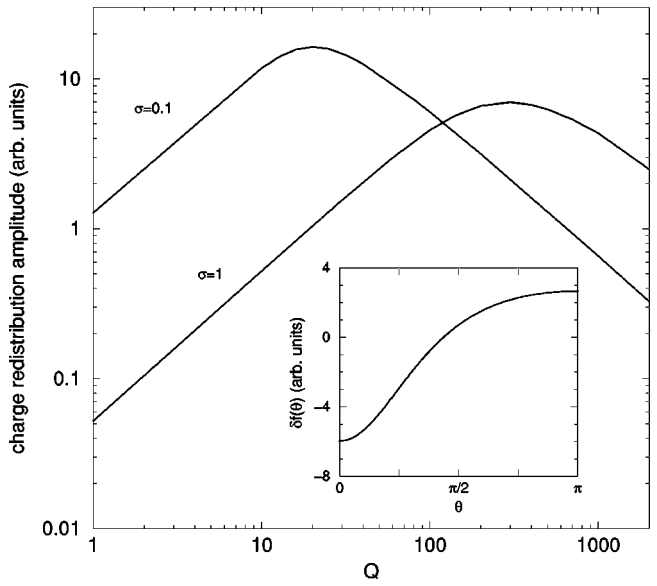

FIG. 7. Amplitude of the charge redistribution as functions of Q. Plotted in the inlet is a typical θ dependence of the charge redistribution (against a positive mean density).

rect and it is indeed seen that the line corresponding to $Q=1$ is very close to the dotted line (which is the linear free energy for two point particles of the same Q). This linear behavior is also found by noting that the free energy scales as Q^2 at small Q at fixed d (not shown here).

At $Q=10$, the nonlinearity starts to affect the free energy so that the ratio $F(Q=10)/F(Q=1)\approx 90$, with a few percent decrease towards lower d. When Q is further increased to 100, first we see that the interaction deviates from the screened-Coulomb form at small separations. Also the free-energy saturates, as apparent in Fig. 5 that the lines corresponding to $Q=100$ and $Q=1000$ are almost indistinguishable.

In the case of constant surface potential in which the surface charges are able to redistribute at different interparicle separations, the free energy should be smaller. Indeed our calculation does find it to be smaller, however, the difference is insignificant and would be indistinguishable if drawn in Fig. 5. The reduction is about 1% at $2d=0.5$ in the linear regime ($Q\lesssim 10$) and becomes even smaller when Q or the particle separation $2d$ increase (see the discussion of Fig. 6 below).

One may think that this small reduction is due to the relatively small particle size at $\sigma=0.1$, and hence the limited range of charge motion. We indeed obtain larger free energy reduction for larger particle sizes. In Fig. 6 we plot the reduction *percentage* of the free energy from the uniform charge to constant potential conditions. For $\sigma=1$ and $Q=1$ we do get a larger change of about 13% at $2d=2.5$ (i.e., a value of 0.5 of the particle surface to surface distance) and the value drops to about 2% at a large separation of $2d=4$. At small Q these values remain approximately independent of Q; a result must hold if the linear Poisson-Boltzmann equation is a good description. On the other hand, when the ion condensation appears at large Q, this difference in free energy quickly drops and approaches zero. This can also been seen from the earlier drop for the smaller particle size $\sigma=0.1$. The reason for this behavior can be seen from Fig. 7 where we plot the charge redistribution δf as functions of Q for both $\sigma=0.1$ and $\sigma=1$. [Since the θ dependence of the redistributions are very similar for different Q and $2d$, only representative amplitudes of $\delta f(\theta)$ are plotted here.] δf scales linearly with Q at small Q, but at large Q even when the average density increases δf decreases and decays to zero. This indicates that at large Q with a condensation region near particle surfaces, only a very small redistribution of charges would restore the constant potential. Hence at high Q with ion condensation which is the main interest in this paper, both boundary conditions would yield very similar results.

The saturation of free energy at high Q for both boundary conditions, however, cannot be solely explained by the satu-

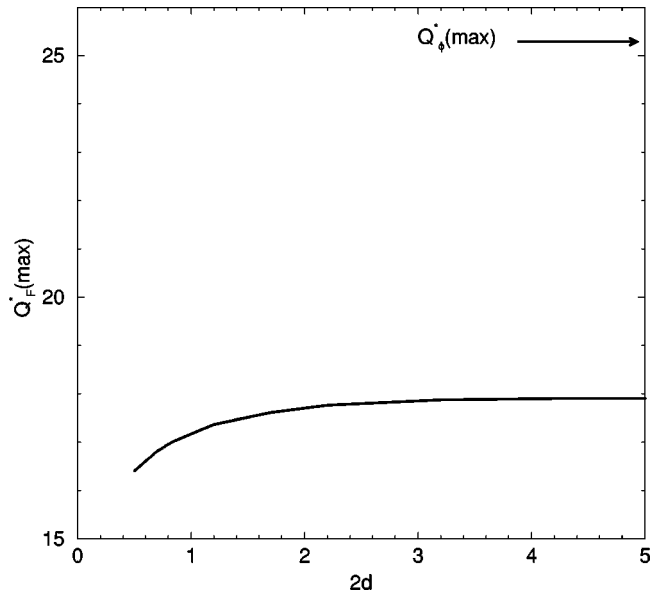

FIG. 8. Maximum effective charge from the two-particle free energy as a function of separation at $\beta=0.5$ and $\sigma=0.1$.

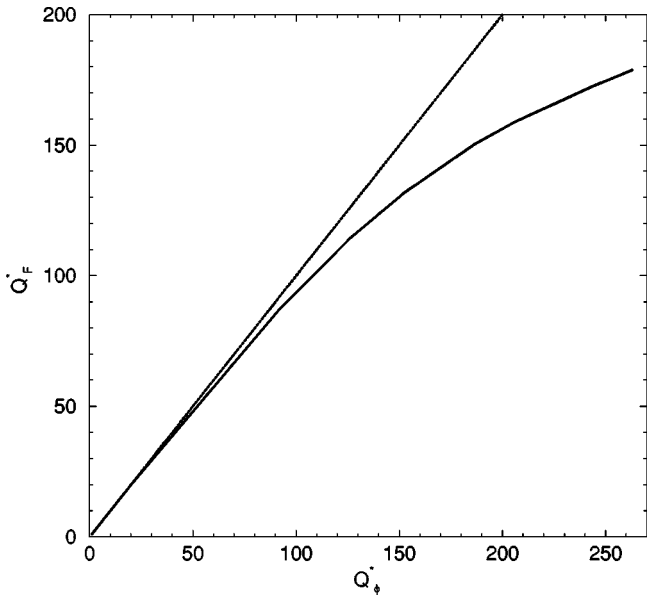

FIG. 9. $Q_F^*(\max, d=2)$ as a function of $Q_\phi^*(\max)$ for $\sigma=1$.

rated far-field single-particle potential discussed in Sec. IV. (We will only show the results for uniform charges from now on.) To see this, we first define another effective charge from the free energy

$$Q_F^*(Q,d) \equiv \lim_{Q_0 \to 0} \left[\frac{F(Q,d)}{F(Q_0,d)} \right]^{1/2} Q_0,$$

and its maximum limiting value $Q_F^*(\max) = Q_F^*(Q \to \infty)$. $Q_F^*(\max)$ is plotted in Fig. 8 for $\beta=0.5$ and $\sigma=0.1$. The arrow near the top of the graph marks the value of $Q_\phi^*(\max)$. At large separations, $Q_F^*(\max)$ approach a constant value, with a significant reduction from $Q_\phi^*(\max)$ [$Q_\phi^*(\max)$ is about 40% higher]. As the particles move closer, there is a further decrease of $Q_F^*(\max)$.

We believe that the reduction of $Q_F^*(\max)$ from $Q_\phi^*(\max)$ is due to the nonlinear interaction inside the condensation region. This can be understood from Fig. 9 in which Q_F^* is plotted against Q_ϕ^* for a range of Q ($\sigma=1$). If the condensated ions were inactive, we should obtain a straight line. Instead, the solid curve in Fig. 9 starts to deviate from the straight line at about $Q_\phi^* \approx 90 (Q \approx 100)$, the value at which the single-particle potential starts to have condensation in Fig. 2.

The maximum values $Q_F^*(\max)$, at a particle surface to surface distance of twice the Debye length, are plotted as a function of the particle size in the lower curve of Fig. 4. The reduction from $Q_\phi^*(\max)$ to $Q_F^*(\max)$ is fairly uniform for all particle sizes, from small particles at 0.05λ to large ones at 8λ.

The decrease of $Q_F^*(\max)$ at small separations also implies that there will be significant many-body corrections to the pair interaction at small separations. This is important since in realistic physical situations usually many particles are spatially confined. These many-body corrections will have the effect of further reducing the effective charges. Better quantitative predictions can only be made if a method to compute the interacting free energy for the multiple-particle systems can be developed.

VI. CONCLUSIONS

Solutions of the Poisson-Boltzmann equation for a charged particle have previously been shown to have a region concentration near the particle surface. The far-field solutions retain the Debye-Hückel form with a renormalized (effective) charge strength. This strength reaches a saturation value at high charges.

From numerical solutions of the PBE for two charged spheres with both uniform charge and constant potential boundary conditions, we have shown that the effective charge obtained from a single-particle far-field solution cannot be used to predict the two-particle interaction strength. The results that we have obtained indicate that at high charges two-particle interactions do not retain the Debye-Hückel form at small separations. The interacting strength measured in terms of the effective charge inferred from the free energy depends on particle separation, and is significantly reduced. The difference is about 40% for all particle sizes. We believe that this reduction is due to the the highly charged condensation regions near each particle, although small, are still actively interacting with the potential from the other particle. We also argue that many-body corrections should further reduce the effective charge.

ACKNOWLEDGMENTS

The authors would like to thank Dr. Jorge Viñals for careful reading of the manuscript. The support of National Science Counsel, Taiwan, through Contract No. NSC 88-2112-M-008-004 is acknowledged.

[1] W. B. Russel, D. A. Saville, and W. R. Schowalter, *Colloidal Dispersions* (Cambridge University Press, Cambridge, England, 1989).

[2] C. K. Goertz, Rev. Geophys. **27**, 271 (1989).

[3] J. H. Chu and Lin I, Phys. Rev. Lett. **72**, 4009 (1994); Physica A **205**, 183 (1994); H. Thomas, G. E. Morfill, V. Demmel, J. Goree, B. Feuerbacher, and D. Mohmann, Phys. Rev. Lett. **73**, 652 (1994); Y. Hayashi and K. Tachibana, Jpn. J. Appl. Phys., Part 1 **33**, 804 (1994).

[4] J. Israelachvili, *Intermolecular & Surface Forces*, 2nd ed. (Academic Press, London, 1992).

[5] See, e.g., D. A. McQuarrie, *Statistical Mechanics* (Harper & Row, New York, 1976), Chap. 15. It is also noted that in some low density rf discharge plasmas the ion mean-free path (determined by the collision rate between ionic and neutral molecules) may be comparable or larger than the Debye length. The validity of the Boltzmann distribution is then in doubt. Nevertheless this assumption is still commonly used in many literatures, and we will consider only this model in this paper.

[6] G. S. Manning, J. Chem. Phys. **51**, 924 (1969).

[7] See, e.g., C. A. Tracy and H. Widom, Physica A **244**, 402 (1997).

[8] G. Senatore and L. Blum, J. Phys. Chem. **89**, 2676 (1985); L. Belloni, J. Chem. Phys. **85**, 519 (1986); S. Khan, T. L. Morton, and D. Ronis, Phys. Rev. A **35**, 4295 (1987).

[9] S. Alexander, P. M. Chaikin, P. Grant, G. J. Morales, and P. Pincus, J. Chem. Phys. **80**, 5776 (1984).

[10] H. Löwen, J.-P. Hansen, and P. A. Madden, J. Chem. Phys. **98**, 3275 (1993).

[11] S. L. Carnie, D. Y. C. Chan, and J. Stankovish, J. Colloid Interface Sci. **165**, 116 (1994). There are also works for unequal particle sizes, S. A. Palkar and A. M. Lenhoff, *ibid.* **165**, 177 (1994), and for a sphere and a plate, J. Stankovich and S. L. Carnie, Langmuir **12**, 1453 (1996).

[12] See, e.g., N. A. Krall and A. W. Trivelpiece, *Principles of Plasma Physics* (McGraw-Hill, New York, 1973), Chap. 1.

[13] A. L. Leob, J. Th. G. Overbeek, and P. H. Wiersema, *The Electrical Double Layer around a Spherical Particle* (MIT Press, Cambridge, MA, 1961).

[14] See, e.g., W.-T. Juan and Lin I, Phys. Rev. Lett. **80**, 3073 (1998).

[15] A rf dusty plasma usually has a value of η very different from 0.5 since normally $T_e \gg T_i$. A common value from a typical plasma experiment with $\eta = 0.01$ would give a similar value of $Q_\phi^*(\max)$ of about 10.